Proc. Natl. Acad. Sci. USA
Vol. 90, pp. 4271–4275, May 1993
Immunology

Three-dimensional structure of a human immunoglobulin with a hinge deletion

LUKE W. GUDDAT*, JAMES N. HERRON†, AND ALLEN B. EDMUNDSON*‡

*Harrington Cancer Center, 1500 Wallace Boulevard, Amarillo, TX 79106; and †Department of Pharmaceutics, University of Utah, Salt Lake City, UT 84108

Communicated by John Roth, January 4, 1993

ABSTRACT **X-ray analysis at 3.2-Å resolution revealed that the Mcg IgG1 (λ chain) immunoglobulin is a compact T-shaped molecule. Because of the hinge deletion, the Fc fragment lobe is pulled tightly upward into the junction of the Fab arms. Along the molecular twofold axis, the Fab arms are joined by an interchain disulfide bond between the two light chains. The antigen combining sites consist of large irregular cavities at the tips of the Fab regions. Potential complement (C1q) binding sites on Fc are sterically shielded by the Fab arms, but putative attachment sites are accessible for docking with the FcRI receptor on human monocytes and with protein A of *Staphylococcus aureus*.**

Progress in the elucidation of three-dimensional structures of intact antibodies has been slow for two principal reasons. (*i*) Supplies of crystalline proteins have been limited, and (*ii*) the Fc units have been disordered in crystals of immunoglobulins containing hinge regions. Like Mcg (1–4), the Dob IgG1 protein has a hinge deletion (5) and an Fc region that appears to be ordered in the crystal lattice (6). In the Kol IgG1, the Fc is disordered, but the structures of the Fab arms and the hinge region are well defined (7, 8). Similarly, a comparison of the Zie IgG2 molecule and its $F(ab)_2$ fragment indicated that the Fc does not contribute significantly to the diffraction pattern of the intact IgG2 protein (9).

The absence of a hinge region is associated with a substantial loss of segmental flexibility in an antibody molecule (10–13). Such a protein is more compact in solution, since sedimentation coefficients increase as hinge regions become shorter (13, 14). Hinge deletions are also accompanied by alterations (or abrogation) of important effector functions such as complement fixation and attachment to cellular receptors (1, 2, 11–20; J. M. Woof and D. R. Burton as quoted in ref. 21).

Unlike most IgGs, the Mcg protein is a euglobulin that can be crystallized by dialysis against deionized water (3). In an earlier study (4), the crystal structure was determined at 6.5-Å resolution by the multiple isomorphous replacement (MIR) method with five heavy-atom derivatives. Individual domains from known structures of human immunoglobulin fragments (8, 22–25) were fitted into the low-resolution map with the program SEARCH (6). Attempts to fit domains in pairs—e.g., variable region light and heavy chain (V_L–V_H) or constant region light and heavy chain (C_L–C_H1) pairs—were not very successful because the quaternary structures in Mcg were different from those in Fab fragments (8, 22), Fc fragments (24), and the Dob immunoglobulin (6). Regions near the midplane, where the C_L domains of the Mcg λ-type light chains converged to be linked by an interchain disulfide bond, were more congested than in the Dob protein. Although the κ-type light chains of Dob were also connected by a disulfide bridge, the structure seemed to be less restrained than Mcg and to have more canonical arrangements of the V and C pairs of domains. Moreover, the Fc region of Dob was built to resemble the structure of the unrestricted Fc fragment where the C_H2 domains are about 20 Å apart (24). In Mcg the C_H2 domains are pulled together at the top by the connections to the Fab arms. Since Mcg appeared to be the odd molecule in the group, it was incumbent upon us to extend the structure to higher resolution. This structure§ and its implications are described in the present report.

METHODS

Collection of X-Ray Diffraction Data and Extension of Phases. The Mcg IgG1 protein crystallized in deionized water (3) in the orthorhombic space group $C222_1$, with a = 88.4, b = 110.0, and c = 186.7 Å. For the present work, a single crystal was used to collect 3.2-Å data at 13°C with a Siemens area detector and a rotating anode operated at 40 kV and 80 mA. These data were 94.5% complete for intensities $I > \sigma(I)$, where σ is the standard deviation based on counting statistics (see Table 1).

With diffractometer data from 8- to 3.5-Å (5132 reflections, 46% complete), the MIR model was previously refined in stages to an R factor of 28% with the program PROLSQ (26). The amino acid sequence of the light chain was provided by Fett and Deutsch (27). D. C. Shaw (personal communication) determined the sequences of residues 1–69 and 109–117 of the V_H domain. The remaining residues in V_H and in the three C_H domains were assigned sequences by comparisons with similar heavy chains (28).

Data from the diffractometer were replaced with the area detector set, and the refinement was continued by the procedure outlined in Table 2. X-PLOR (29) was used for rigid-body refinement, first with the Fab and Fc regions treated as intact units and then with six individual domains. The R factor for the 10- to 4-Å set (99% complete) was 46.9%. Small rotations and translations from their starting positions were noted for all domains, but especially for C_L. X-PLOR was next used for positional refinement (600 cycles) and simulated annealing ("slow-cooling" protocol) with 10- to 3.5-Å data. To reduce the effects of model bias, the three complementarity-determining regions (CDR) of the heavy chain, the segment connecting the C_H2 and C_H3 domains, and the carbohydrate were not included in the model used for the initial stage of positional refinement. These segments were then located by difference Fourier analyses and added to the model. As a further precaution, the structures of these segments were rebuilt after calculation of "annealed omit" maps (29).

The publication costs of this article were defrayed in part by page charge payment. This article must therefore be hereby marked "*advertisement*" in accordance with 18 U.S.C. §1734 solely to indicate this fact.

Abbreviations: MIR, multiple isomorphous replacement; V_L, V_H, C_L, and C_H, light and heavy chain variable and constant regions.

‡To whom reprint requests should be addressed.

§The atomic coordinates and structure factors have been deposited in the Protein Data Bank, Chemistry Department, Brookhaven National Laboratory, Upton, NY 11973 (reference 1MCO, 1MCOSF). Information on coordinates is available immediately; information on structure factors is embargoed for one year from the date of publication.

Table 1. Crystallographic and diffraction data for Mcg IgG1 (λ chain)

Shell, Å	Unique reflections		% obs./theor.	Measurements, no.	R_{merge},* %
	Obs.	Theor.			
∞–3.20	14,525	15,365	94.5	43,520	14.79

The diffraction data were collected with a Siemens area detector on a crystal of orthorhombic space group $C222_1$ with a = 88.4, b = 110.0, and c = 186.7 Å. Reflections were considered observed (Obs.) if the intensity $I > \sigma(I)$, where σ is the standard deviation. Theor., theoretical.
*R_{merge} is the unweighted-squared R factor on intensity × 100.

To complete the procedure, cycles of refinement were alternated with interactive model building on a Silicon Graphics IRIS 4D/80GT graphics workstation with the program TURBO-FRODO (30, 31). $F_o - F_c$ OMIT maps (32) were calculated with 20 of 642 residues deleted at each step until the entire asymmetric unit was examined and rebuilt as necessary. Dihedral angles were checked with "Ramachandran plots" (31). Residues with ϕ and ψ angles outside the prescribed boundaries were refitted and subjected to additional refinement cycles. Currently, the R factors are 21.5% at 3.5-Å and 23.2% at 3.2-Å resolution. Root-mean-square (rms) deviations from ideal values are 0.022 and 0.027 Å for bond lengths and angles.

Molecular Replacement Methods. An attempt was made to solve the structure independently by molecular replacement methods (33–35). Rotation, translation, and correlation functions were calculated with the programs MERLOT (33) and RTMAP (35) with 8- to 4- or 6- to 4-Å data. V_L–V_H, C_L–C_H1 and C_H2–C_H3 pairs of domains from the Kol and New Fabs (8, 22) and the human Fc (24) were selected as starting models. Individual domains, including those of the Mcg light chain (25), were subsequently used as probes. For comparison, the same procedures were applied to a light–heavy chain (L–H) combination and to V_L–V_H, C_L–C_H1, and C_H2–C_H3 pairs taken from the present crystal structure.

Models for the Carbohydrate Moieties. Atomic coordinates for the carbohydrate in human Fc (24) were rotated and translated into equivalent positions in the Mcg structure. Cycles of X-PLOR refinement, model building, and calculations of OMIT maps were continued until the carbohydrate structures stabilized. The envelope of electron density for the α(1,6) carbohydrate branch contained an extra module shaped like *N*-acetylneuraminic (sialic) acid. After this residue was added, its presence was confirmed by inspection of all subsequent OMIT maps.

RESULTS AND DISCUSSION

Structural Determination and Description of the Molecule. After refinement at 3.2-Å resolution (Table 2), the polypeptide chains could be traced throughout their lengths, and >95% of the side chains could be fitted to the electron density. To illustrate the quality of the maps, a stereo diagram of "cage" electron density for a light chain segment (residues 30–36) is presented with a superimposed skeletal model in Fig. 1.

As an independent approach to the structural analysis, molecular replacement techniques were not effective with canonical pairs of domains as starting models. Among single-domain probes, only V_L from the Mcg light chain dimer (25) gave interpretable results. When the search models consisted of the entire L–H asymmetric unit, the V_L–V_H pair, or the C_L–C_H1 pair extracted from the present IgG1 structure, however, the predicted orientations accounted for the highest peaks in the maps. With the C_H2–C_H3 probe, the correct orientation was represented by the fourth highest peak.

In another test of the plausibility of the present structure, the locations of 35 sites occupied by heavy atoms in the MIR study (4) were codisplayed with the atomic model of the protein. Without exception, the heavy atom positions followed the molecular envelope of the protein in chemically compatible sites.

A RIBBONS model (36) of the IgG1 protein is shown in Fig. 2 with color-coded β-pleated sheets. The molecule spans 148 Å from tip to tip of the Fab arms (distance measured between the α-carbons of the two light chain serine-27 residues;

Table 2. Refinement protocol and statistics for data in Table 1

Program	Resolution, Å	No. of Fs, $I > 2\sigma(I)$ (% obs.)	R_c, %	Δd, Å	
				Distance	Angle
X-PLOR					
2 rigid bodies	20–10	478 (99.1)	52.4	—	—
6 rigid bodies	10–7	1,008 (99.6)	46.7	—	—
6 rigid bodies	10–6	1,891 (99.6)	45.2	—	—
6 rigid bodies	10–5	3,595 (99.7)	45.9	—	—
6 rigid bodies	10–4	7,407 (99.3)	46.9	—	—
600 cycles of positional X-PLOR	10–3.5	11,030 (97.8)	27.2	0.035	0.040
S.A. to 3000 K	10–3.5	11,030 (97.8)	23.5	0.030	0.038
S.A., model build	10–3.5	11,030 (97.8)	23.0	0.029	0.037
	8–3.2	13,184 (94.7)	24.5	0.029	0.035
PROLSQ	10–3.5	11,030 (97.8)	21.5	0.040	0.060
	10–3.2	13,481 (92.8)	24.3	0.022	0.027
	6–3.2	11,875 (91.8)	23.2	0.022	0.027

S.A., simulated annealing; obs., observed; Fs, structure factors; R_c, crystallographic R factor; Δd, rms deviations in bond lengths and angles.

Cumulative orientation shifts of domains from 20- to 10-Å resolution through 10- to 4-Å resolution are as follows:

	$\phi°_X$	$\phi°_Y$	$\phi°_Z$	ΔX	ΔY	ΔZ		$\phi°_X$	$\phi°_Y$	$\phi°_Z$	ΔX	ΔY	ΔZ
V_L	−3.7	0.3	−1.0	−0.85	−1.40	−2.80	C_H1	−4.7	3.8	−3.2	1.50	0.70	0.20
V_H	1.3	5.0	1.8	1.80	−2.10	1.20	C_H2	−0.7	−6.9	−2.1	0.00	2.30	−0.90
C_L	−4.0	−5.4	6.4	−0.90	−1.50	1.00	C_H3	0.1	1.5	−2.2	−0.30	−0.70	−0.70

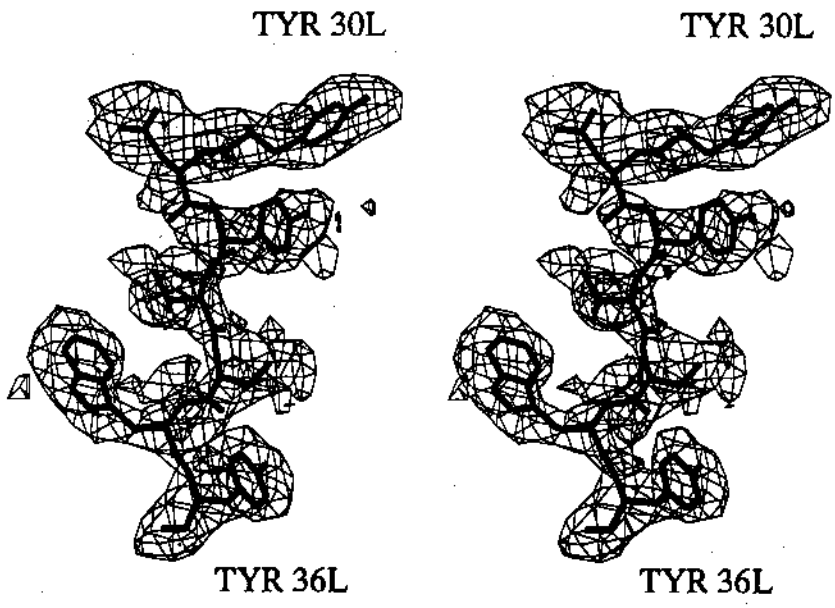

FIG. 1. Stereo diagram of the three-dimensional "cage" electron density for residues 30–36 of the Mcg light chain (Tyr-30L to Tyr-36L) with the skeletal model superimposed. The sequence is Tyr-Asn-Tyr-Val-Ser-Trp-Tyr. Residues on the right side of the chain protrude into the antigen combining site.

residues in light and heavy chains will be distinguished henceforth by L or H and the position juxtaposed). Each V_L domain extends about 4 Å beyond the outer boundary of the heavy chain. From top to bottom, the molecule measures about 95 Å along *y*, the crystallographic and molecular dyad that bisects the disulfide bond between the two light chains. The y-axis also passes between the two halves of the Fc region, which is about 65 Å long and 65 Å across in its widest dimension. Solvent is estimated (4) to occupy about 61% of the crystal volume. In addition to the external pockets, large solvent cavities are found within each molecule: e.g., in the interface of V_L and V_H (the antigen combining site), in the space between V and C pairs, between the light chain junction and Fc, between the C_H2 domains, and between C_H2 and C_H3.

FIG. 2. RIBBONS model (36) illustrating the secondary and tertiary structure of the Mcg IgG1 immunoglobulin together with its N-linked oligosaccharides. One asymmetric unit (a light chain and a heavy chain) is represented by yellow tubular backbone segments with color-coded ribbons to designate strands of β-pleated sheets. The second asymmetric unit has white tubular backbone segments. In the V domains (far right and far left at the top) the five-stranded β-pleated sheets are colored green and cyan in the heavy chains and grey in the light chains. Three-stranded sheets in the C domains have the same color code as the five-chain layers in the V domains. Four-stranded layers are orange and rose in the heavy chains and dark blue in the light chains. Oligosaccharide models in the Fc region are shown as groups of pink or red spheres. The disulfide bond between the penultimate residues of the two light chains is represented by a yellow ball and stick model.

It is interesting to consider how the Mcg IgG1 components differ from canonical structures of Fab and Fc fragments. These differences are accentuated in the "elbow-bend" angle, the pseudosymmetry between domain pairs, and the quaternary structures. The elbow-bend angle, defined as the angle subtended by the pseudo-twofold axes of rotation between pairs of V and C domains, is 118° in the Mcg Fab. This angle is smaller than those of the human New (135°), Dob (147°), and Kol (174°) Fabs (6, 8, 22) as well as those in numerous murine Fabs (34–35, 37–39). It is bracketed between the elbow-bend angles for the trigonal (115°) and orthorhombic (132°) forms of the Mcg light chain dimer (25), which resembles a typical Fab more closely than the authentic Fab in the IgG1 protein.

The pseudo-twofold symmetry between pairs of domains was examined by comparing sets of α-carbon atoms from conserved parts of the β-pleated sheets. When 38 pairs of these atoms (listed in ref. 23) were compared with the program ROTMOL (supplied by W. Steigemann and R. Huber), V_L could be brought into coincidence with V_H by a rotation of only 161°. With 34 pairs of atoms from the C domains, a rotation angle of only 153° was required to superimpose C_L on C_H1. Pseudo-twofold angles calculated for the more typical BV04-01 Fab (35) and the Mcg light chain dimer (25) were 174° and 180° for the V pairs and 170° and 180° for the C pairs. Calculations for other Fabs clustered around these more common values.

In comparisons of quaternary structures, the five-stranded β-pleated sheet of V_L was found to face the corresponding sheet in V_H, as in other immunoglobulins (see Fig. 2). Likewise, the four-stranded sheets meet along the interface of C_L and C_H1 as expected. Relative to canonical pairs, however, the sheets in Mcg have had to rotate and slide along the articulating surfaces to adjust to the combination of a hinge deletion and the —S—S— cross-linking of the light chains.

V_L and V_H form a loosely packed dimer stabilized by 94 interatomic contacts involving only seven residues of the

light and eight residues of the heavy chain. In this article two atoms are considered to be in contact if they are separated by <4 Å, which is the sum of van der Waals radii plus a tolerance of ≈0.4 Å. The active site between V_L and V_H is a large, irregular cavity 16 to 23 Å across and 14 to 22 Å deep. Because of the loose packing, the cavity is not sealed at its base. It is continuous with a tunnel (4–10 Å in diameter), which extends to the solvent space between the V and C domain pairs. Phenylalanine L98 interacts with tryptophan H47 at the beginning of the tunnel, but the remainder is not bridged by any side chains. On one side the tunnel is composed of residues identical to those lining the walls of the deep binding pocket (23) of the Mcg light chain dimer (proline-L44, tyrosine-L87, and glutamine-L38, front to back). Heavy chain components on the opposite side are leucine-H45, tyrosine-H91, and glutamine-H39. At the end of the tunnel the shortest distance between glutamines at positions L38 and H39 is 11.4 Å, in sharp contrast to the 2.8-Å separation of the L38 pair of glutamines that terminate the deep pocket in the light chain dimer. The presence of such a large cavity is unusual among known Fabs (38, 39), and a tunnel has not yet been seen elsewhere. Both the cavity and tunnel are available for ligand binding. In addition to the customary mode of entry, an alternate route to the tunnel is open to small ligands through the solvent reservoir between the V and C pairs.

Unlike the V domains, C_L and C_H1 associate closely to produce a dimer with many (277) interdomain contacts, divided among 22 light and 18 heavy chain residues. Deviations from canonical pairing involve rigid-body shifts of both domains and conformational changes in individual segments. While C_L and C_H1 intersect at approximately the same angle as the C_L domains of the light chain dimer (93° vs. 95°), the predominant directions of the domains have changed in the IgG1. C_L slants upward toward the second light chain and C_H1 slopes downward toward the connector to C_H2 (see Fig. 2). In a typical IgG1 antibody, the hinge segment joined to C_H1 forms a disulfide bond with the light chain and thus holds the ends of C_H1 and C_L in close proximity.

An additional alteration occurs in the orientation expected for C_L. Using a light chain from the Mcg dimer as a canonical structure, we superimposed its V_L on the V_L in IgG1 and then compared the C_L domains. The center of mass of C_L in the IgG1 protein was found to be translated 15 Å relative to its position in the light chain dimer. This translation was mediated mainly through the "switch region" between V_L and C_L. Such extensive adjustments were made without seriously compromising the complementarity of C_L with C_H1.

C_H1 is connected to the C_H2 domain on the opposite side of the crystallographic twofold axis (a trans relation). A cis type of connectivity is incompatible with the electron density. Since the last residue (valine-H215) in C_H1 remains associated with the globular part of the domain, the connector is derived exclusively from the C_H2 sequence Ala-Pro-Glu-Leu-Leu-Gly-Gly. To avoid confusion, the residues are numbered 231–237 as in other antibodies. In functioning as a hinge by-pass, this heptapeptide segment assumes an almost fully extended conformation (23 Å in length) in a solvent trough about 9 Å deep and 16 Å across in its widest dimension.

When locked into the Mcg molecule, the Fc unit adopts a different quaternary structure than that found in unrestrained Fc fragments (24, 40). In Mcg the C_H2 domains approach each other closely (5.0 Å) at an angle of 113° at the top of the Fc unit. The taut hinge-bypass segments act as tethers that pull the C_H2 domains toward the midplane. This movement leads to a bend angle of 67° at the junction of C_H2 and C_H3. Whereas the C_H2 domains in Mcg are related by a crystallographic twofold axis, their orientations are not strictly symmetrical in Fc fragments. Moreover, the bend angle at the C_H2–C_H3 junction is 89° in one subunit of the human Fc fragment and 92° in the second (24).

In Mcg the C_H3 domains cross each other at a wider angle than in the Fc fragment (119° vs. 108°). Along the articulating surfaces of the two domains in Mcg there are 200 interatomic contacts. Pairing interactions between the C_H3 domains are generally considered to be the dominant noncovalent forces holding an IgG1 molecule together (association constant of 10^{10} M^{-1} (41).

Oligosaccharides Linked to the C_H2 Domains. At least 30 types of N-linked oligosaccharides have been demonstrated in IgG samples from human sera (42). In rabbit Fc the carbohydrates are asymmetric in both sequence and structure (40). Chemical analyses of Mcg samples used in crystallization trials gave nonintegral molar ratios for the monosaccharides, a strong indication of heterogeneity. In the molecules actually incorporated into crystals, however, the oligosaccharides are related by twofold symmetry, with its implied suggestion of homogeneity.

Instead of participating in interactions like those observed in the rabbit Fc (40), the α(1,3) carbohydrate arms (disaccharides of mannose and *N*-acetylglucosamine) in Mcg face each other across the midplane of the molecule without touching. The bridge sugar (*N*-acetylglucosamine) linked to asparagine H297 and the adjacent L-fucose residue remain close to the protein and interact with tyrosine-H296 and asparagine-H297. After the mannose core structure, the last three units in the α(1,6) branch (*N*-acetylglucosamine, galactose, and sialic acid) cross segments 1, 2, and 3 of the four-stranded β-pleated sheet and weakly interact with the protein.

Functional Implications of the IgG1 Structure. Although the natural antigen is unknown, the Mcg IgG1 protein was found (43) to bind peptides synthesized on solid supports by the method of Geysen *et al.* (44). Like Dob and Lec (11), Mcg failed to fix complement (1, 2) but did show binding activity for protein A of *Staphylococcus aureus* (E. M. Preston and A.B.E., unpublished work) and for the high-affinity Fc

FIG. 3. Stereo diagram showing the heptapeptide (hinge bypass) segment connecting C_H1 (domain in upper right) and C_H2 (domain in lower left) of one heavy chain (in blue). The sequence of the connector, derived exclusively from the C_H2 gene product, is Ala-Pro-Glu-Leu-Leu-Gly-Gly (residues 231–237). Side chains are presented as green spheres, except for Leu-235, which is white. Leu-235 is believed to be a key residue in the attachment site for the high-affinity Fc receptor on human monocytes (19, 23). The symmetry-related components of the second heavy chain are shown in red. Intrachain disulfide bonds are colored yellow.

receptor (FcRI) on human monocytes (J. M. Woof and D. R. Burton as quoted in ref. 21).

The structure shown in Fig. 2 is compatible with the view (11) that the docking of complement component C1q is obstructed by the Fab arms in IgG proteins without hinge regions. A critical part of the docking site on C_H2 includes glutamic acid-H318, lysine-H320, and lysine-H322 (20). In Mcg this site is accessible from below, but the lateral approaches are restricted by the V_L domains, and the access routes from above are blocked by C_H1 from the opposite heavy chain.

Note that only one potential binding site for C1q is present on the "front" face of the molecule displayed in Fig. 2. Since the symmetry-related site is sterically segregated on the "back" face, it is necessary to have two IgG molecules side by side to accommodate the minimal binding unit (two of six "heads") of C1q. This geometric arrangement probably explains why IgG antibodies have to be aggregated before they can activate the complement cascade.

As a consequence of the tilting of C_H2 in Mcg, the space available for protein A binding at the C_H2–C_H3 junction is even larger than that in the Fc fragment (24). For example, the distances between the α-carbons of methionine-H252 on C_H2 and histidine-H435 on C_H3 are 15.3 Å in Mcg and 7.9 Å in Fc.

The putative binding site for FcRI, centered around leucine-H235 (16, 17) in the hinge-bypass segment, is illustrated in Fig. 3. Such an accessible, but semiprotected environment should meet the selectivity criteria for high-affinity binding to Fc receptors. As in C1q docking sites, the symmetry-related heptapeptide segments are located on different faces of the Mcg molecule and therefore can function as two independent sites for receptor attachment.

With viable ligand combining sites in the Fab arms and receptor attachment sites in the Fc region, the Mcg IgG1 molecule seems to be a prototype for an unusual but not abnormal class of functional immunoglobulins. We prefer to consider it as a molecule representing one end of the enormously diverse set of antibodies that can be generated by the immune system.

This article is dedicated to Professor Harold F. Deutsch, who first crystallized the Mcg protein and explained its significance. This work was supported by Grant CA 19616, awarded by the National Cancer Institute, and by the Harrington Cancer Center. We thank Leif Hanson and Bryan Schley for many helpful discussions and Twyla Slay for preparing the manuscript for publication.

1. Deutsch, H. F. & Suzuki, T. (1971) *Ann. N.Y. Acad. Sci.* **190,** 472–486.
2. Fett, J. W., Deutsch, H. F. & Smithies, O. (1973) *Immunochemistry* **10,** 115–118.
3. Edmundson, A. B., Wood, M. K., Schiffer, M., Hardman, K. D., Ainsworth, C. F., Ely, K. R. & Deutsch, H. F. (1970) *J. Biol. Chem.* **245,** 2763–2764.
4. Rajan, S. S., Ely, K. R., Abola, E. E., Wood, M. K., Colman, P. M., Athay, R. J. & Edmundson, A. B. (1983) *Mol. Immunol.* **20,** 787–799.
5. Steiner, L. A. & Lopes, A. D. (1979) *Biochemistry* **18,** 4054–4067.
6. Silverton, E. W., Navia, M. A. & Davis, D. R. (1977) *Proc. Natl. Acad. Sci. USA* **74,** 5140–5144.
7. Colman, P. M., Deisenhofer, J., Huber, R. & Palm, W. (1976) *J. Mol. Biol.* **100,** 257–278.
8. Marquart, M., Deisenhofer, J., Huber, R. & Palm, W. (1980) *J. Mol. Biol.* **141,** 369–392.
9. Ely, K. R., Colman, P. M., Abola, E. E., Hess, A. C., Peabody, D. S., Parr, D. M., Connell, C. E., Laschinger, C. A. & Edmundson, A. B. (1978) *Biochemistry* **17,** 820–823.
10. Ygueramide, J., Epstein, H. F. & Stryer, L. (1970) *J. Mol. Biol.* **51,** 573–590.
11. Klein, M., Haeffner-Cavaillon, N., Isenman, D. E., Rivat, C., Navia, M. A., Davies, D. R. & Dorrington, K. J. (1981) *Proc. Natl. Acad. Sci. USA* **78,** 524–528.
12. Oi, V. T., Vuong, T. M., Hardy, R., Reidler, J., Dangl, J., Herzenberg, L. A. & Stryer, L. (1984) *Nature (London)* **307,** 136–140.
13. Burton, D. R. (1985) *Mol. Immunol.* **22,** 161–206.
14. Gregory, L., Davis, K. G., Sheth, B., Boyd, J., Jefferis, R., Nave, C. & Burton, D. R. (1987) *Mol. Immunol.* **24,** 821–829.
15. Yasmeen, D., Ellerson, J. R., Dorrington, K. J. & Painter, R. H. (1976) *J. Immunol.* **116,** 518–522.
16. Woof, J. M., Partridge, L. J., Jefferis, R. & Burton, D. R. (1986) *Mol. Immunol.* **23,** 319–330.
17. Duncan, A. R., Woof, J. M., Partridge, L. J., Burton, D. R. & Winter, G. (1988) *Nature (London)* **332,** 563–564.
18. Isenman, D. E., Dorrington, K. J. & Painter, R. H. (1975) *J. Immunol.* **114,** 1726–1729.
19. Wallick, S. C., Kabat, E. A. & Morrison, S. L. (1988) *J. Exp. Med.* **168,** 1099–1109.
20. Duncan, A. R. & Winter, G. (1988) *Nature (London)* **332,** 738–740.
21. Burton, D. R. (1990) in *Fc Receptors and the Action of Antibodies*, ed. Metzger, H. (Am. Soc. for Microbiol., Washington, DC).
22. Poljak, R. J., Amzel, L. M., Chen, B. L., Phizackerley, R. P. & Saul, F. (1974) *Proc. Natl. Acad. Sci. USA* **71,** 3340–3444.
23. Edmundson, A. B., Ely, K. R., Abola, E. E., Schiffer, M. & Panagiotopoulos, N. (1975) *Biochemistry* **14,** 3953–3961.
24. Deisenhofer, J. (1981) *Biochemistry* **20,** 2361–2370.
25. Ely, K. R., Herron, J. N., Harker, M. & Edmundson, A. B. (1989) *J. Mol. Biol.* **210,** 601–615.
26. Hendrickson, W. A. (1985) *Methods Enzymol.* **115,** 252–270.
27. Fett, J. W. & Deutsch, H. F. (1974) *Biochemistry* **13,** 4102–4114.
28. Kabat, E. A., Wu, T. T., Perry, H. M., Gottesman, K. S. & Foeller, C. (1991) *Sequences of Proteins of Immunological Interest* (U.S. Dept. of Health and Human Services, Public Health Service, National Institutes of Health, Bethesda, MD), 5th Ed.
29. Brünger, A. T., Karplus, M. & Petsko, G. A. (1989) *Acta Crystallogr. Sect. A* **45,** 50–61.
30. Jones, T. A. (1978) *J. Appl. Crystallogr.* **11,** 268–272.
31. Roussel, A. & Cambillau, C. (1989) in *Silicon Graphics Geometry Partner Directory (Fall 1989) Silicon Graphics* (Silicon Graphics, Mountain View, CA), pp. 77–78.
32. Bhat, T. N. & Cohen, G. H. (1978) *J. Appl. Crystallogr.* **11,** 268–272.
33. Fitzgerald, P. M. D. (1988) *J. Appl. Crystallogr.* **21,** 273–278.
34. Herron, J. N., He, X. M., Mason, M. L., Voss, E. W., Jr., & Edmundson, A. B. (1989) *Proteins Struct. Funct. Genet.* **5,** 271–280.
35. Herron, J. N., He, X. M., Ballard, D. W., Blier, P. R., Pace, P. E., Bothwell, A. L. M., Voss, E. W., Jr., & Edmundson, A. B. (1991) *Proteins Struct. Funct. Genet.* **11,** 159–175.
36. Carson, M. & Bugg, C. (1986) *J. Mol. Biol.* **4,** 121–122.
37. Amit, A. G., Mariuzza, R. A., Phillips, S. E. V. & Poljak, R. J. (1986) *Science* **233,** 747–753.
38. Colman, P. M. (1988) *Adv. Immunol.* **43,** 99–132.
39. Davies, D. R., Padlan, E. A. & Sheriff, S. (1990) *Annu. Rev. Biochem.* **59,** 439–473.
40. Sutton, B. J. & Phillips, D. C. (1983) *Biochem. Soc. Trans.* **11,** 130–132.
41. Dorrington, K. J. (1978) *Can. J. Biochem.* **56,** 1087–1101.
42. Parekh, R. B., Dwek, R. A., Sutton, B. J., Fernandes, D. L., Leung, A., Stanworth, D. & Rademacher, T. W. (1985) *Nature (London)* **316,** 452–457.
43. Tribbick, G., Edmundson, A. B., Mason, T. J. & Geysen, H. M. (1989) *Mol. Immunol.* **26,** 625–635.
44. Geysen, H. M., Rodda, S. J., Mason, T. J., Tribbick, G. & Schoofs, P. G. (1987) *J. Immunol. Methods* **102,** 259–274.